

The oxygen vacancy effect on the magnetic property of the LaMnO_{3-δ} thin films

Ruiqiang Zhao, Kuijuan Jin, Zhongtang Xu, Haizhong Guo, Le Wang et al.

Citation: *Appl. Phys. Lett.* **102**, 122402 (2013); doi: 10.1063/1.4798550

View online: <http://dx.doi.org/10.1063/1.4798550>

View Table of Contents: <http://apl.aip.org/resource/1/APPLAB/v102/i12>

Published by the [American Institute of Physics](http://www.aip.org).

Related Articles

Three-dimensional mapping of the anisotropic magnetoresistance in Fe₃O₄ single crystal thin films
J. Appl. Phys. **113**, 17B103 (2013)

Magnetic stability of ultrathin FeRh films
J. Appl. Phys. **113**, 17C107 (2013)

The low-frequency alternative-current magnetic susceptibility and electrical properties of Si(100)/Fe₄₀Pd₄₀B₂₀(X Å)/ZnO(500Å) and Si(100)/ZnO(500Å)/Fe₄₀Pd₄₀B₂₀(YA) systems
J. Appl. Phys. **113**, 17B303 (2013)

Interface-controlled magnetism and transport of ultrathin manganite films
J. Appl. Phys. **113**, 17C711 (2013)

First observation of magnetoelectric effect in M-type hexaferrite thin films
J. Appl. Phys. **113**, 17C710 (2013)

Additional information on *Appl. Phys. Lett.*

Journal Homepage: <http://apl.aip.org/>

Journal Information: http://apl.aip.org/about/about_the_journal

Top downloads: http://apl.aip.org/features/most_downloaded

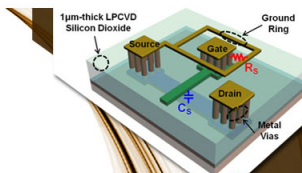
Information for Authors: <http://apl.aip.org/authors>

ADVERTISEMENT



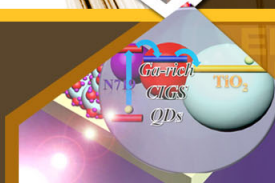
**EXPLORE WHAT'S
NEW IN APL**

SUBMIT YOUR PAPER NOW!



SURFACES AND INTERFACES

Focusing on physical, chemical, biological, structural, optical, magnetic and electrical properties of surfaces and interfaces, and more...



ENERGY CONVERSION AND STORAGE

Focusing on all aspects of static and dynamic energy conversion, energy storage, photovoltaics, solar fuels, batteries, capacitors, thermoelectrics, and more...

The oxygen vacancy effect on the magnetic property of the $\text{LaMnO}_{3-\delta}$ thin films

Ruiqiang Zhao, Kuijuan Jin,^{a)} Zhongtang Xu, Haizhong Guo, Le Wang, Chen Ge, Huibin Lu, and Guozhen Yang

Beijing National Laboratory for Condensed Matter Physics, Institute of Physics, Chinese Academy of Sciences, Beijing 100190, China

(Received 28 January 2013; accepted 13 March 2013; published online 26 March 2013)

The magnetic property of the $\text{LaMnO}_{3-\delta}$ films was systematically investigated with the variation of the deposited oxygen pressure. The Curie temperature and the saturation magnetization of the films were found increased with the decrease of the oxygen pressure. We believe that the double exchange effect between Mn^{2+} and Mn^{3+} ions should be the origin of the ferromagnetism and the enhanced conductivity, where the Mn^{2+} ions are generated with the oxygen vacancies due to oxygen deficient, and the double-exchange interaction is enhanced with increasing the ratio of $\text{Mn}^{2+}/\text{Mn}^{3+}$. The results of the x-ray absorption spectroscopy support our conclusion as well. © 2013 American Institute of Physics. [<http://dx.doi.org/10.1063/1.4798550>]

Oxygen vacancies play a very important role in the properties of transition metal oxides, such as resistive switching characteristics,^{1,2} photoluminescence,^{3–5} high-temperature ferromagnetism,^{6,7} catalysis,⁸ and superconductivity.^{9,10} The LaMnO_3 , as the parent material of the doped manganites, has attracted considerable attentions due to its fantastic properties,¹¹ such as photo-induced infrared absorption,¹² pressure-induced insulator-to-metal transition,¹³ and dielectric anomaly.¹⁴ Oxygen nonstoichiometry in LaMnO_3 was also investigated by many groups, and the magnetic structures of $\text{LaMnO}_{3+\delta}$ (excess-oxygen condition) exhibit the ferromagnetism, spin-glass state, or antiferromagnetism when δ is at different regions.^{15–18} Most of the work has been reported on the origin of the ferromagnetic property, and it was considered that double-exchange interaction^{16,19} and Jahn-Teller distortions^{20–22} are responsible for their ferromagnetism. The properties of the oxygen-deficient case have also been investigated, and another magnetic phase was found in the powder $\text{LaMnO}_{3-\delta}$.²³ However, the influence of oxygen vacancies on the transport and magnetic properties of the LaMnO_3 in the thin-film system has not yet been explored, and the understanding of the relative underlying physics still remains unknown. Recently, our group has reported that the oxygen vacancies play a very important role on the resistive switching phenomenon in the LaMnO_3 films, and the resistive switching property becomes more pronounced with more oxygen vacancies in the films.²⁴ In this work, the structures, transport properties, magnetic properties, and the valence of the Mn ions of the oxygen-deficient $\text{LaMnO}_{3-\delta}$ films have been investigated. Unexpected hysteresis loops were observed in the $\text{LaMnO}_{3-\delta}$ films with oxygen vacancies, and an increase trend of the saturation magnetization of films was observed with the decrease of the deposited oxygen pressure, which was quite different from the well known anti-ferromagnetic property of LaMnO_3 in bulk systems.²⁵ The results of

x-ray absorption near edge spectroscopy showed that the oxidation state of Mn ions changes from +3 to +2 due to oxygen deficiency, and the ratio of $\text{Mn}^{2+}/\text{Mn}^{3+}$ increases with the decrease of the deposited oxygen pressures, inducing the enhancement of the saturation magnetization and the conductivity of the $\text{LaMnO}_{3-\delta}$ heterostructures resulting from the enhancement of double-exchange interaction.

The 100-nm-thick $\text{LaMnO}_{3-\delta}$ films were deposited on SrTiO_3 (001) (0.8 wt. % Nb-doped) (SNT0) substrates by the laser molecular beam epitaxy (Laser-MBE) using a pulsed XeCl excimer laser (308 nm, $\sim 1.5 \text{ J/cm}^2$, 2 Hz) at 750 °C under different oxygen pressures of 10, 5×10^{-1} , 5×10^{-2} , 5×10^{-3} , and 5×10^{-4} Pa, respectively. The crystal structure of the $\text{LaMnO}_{3-\delta}$ films was investigated by the high-resolution synchrotron x-ray diffractometry (SXR) ($\lambda = 1.24 \text{ \AA}$) at BL14B1 beamline of Shanghai Synchrotron Radiation Facility (SSRF). The x-ray absorption near edge spectra (XANES) of the K-edge of Mn ions were measured at BL14W1 beamline of SSRF using fluorescence measurements, and the $L_{II,III}$ -edge spectra were probed at BL08U beamline of SSRF using the Total Electron Yield (TEY) method. The magnetic properties of the $\text{LaMnO}_{3-\delta}$ films were investigated by the physical property measurement system (PPMS, Quantum design). The current-voltage (I - V) behaviors of the $\text{LaMnO}_{3-\delta}$ /SNT0 heterojunctions were measured by a Keithley 2400 source meter at room temperature.

Figure 1 shows the SXR results of the $\text{LaMnO}_{3-\delta}$ films grown under the different oxygen pressures. The SXR results shown in Figs. 1(a)–1(e) reveal that only peaks from the (001) diffraction of the SNT0 and the $\text{LaMnO}_{3-\delta}$ are observed, and no diffraction peaks from secondary phases or randomly oriented grains are observed, indicating that the thin films are grown along the c -axis with a good single phase. It is obviously seen from Fig. 1(f) that the c -axis lattice constants of the films monotonously increase with decreasing the deposited-oxygen-pressure from 10 to 5×10^{-4} Pa. Since the decrease of deposited oxygen pressure results in the

^{a)} Author to whom correspondence should be addressed. Electronic mail: kjjin@iphy.ac.cn

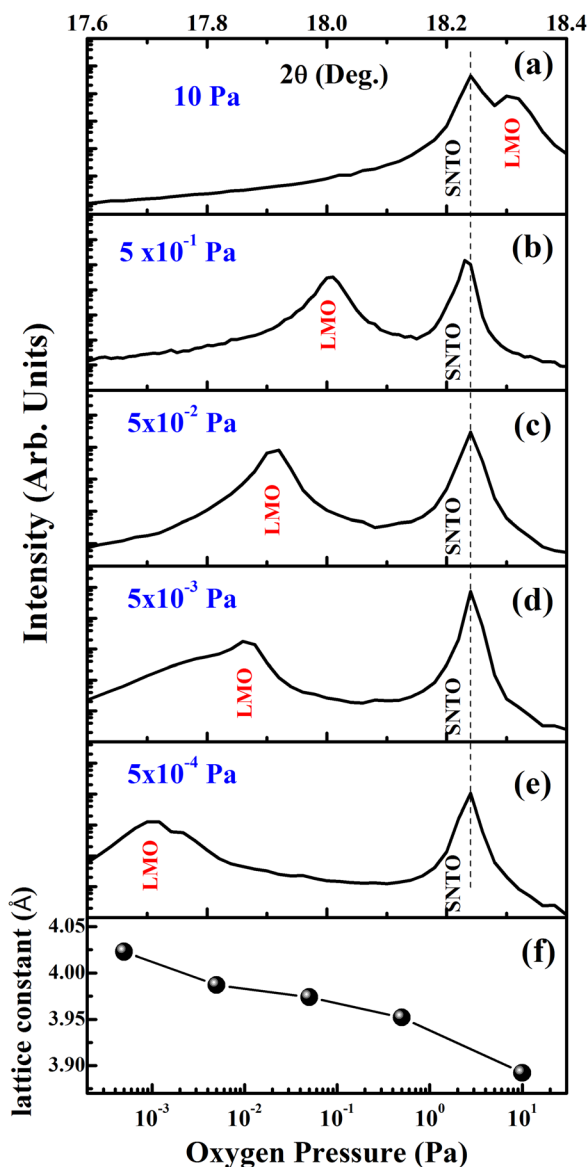


FIG. 1. The SXR D patterns of the $\text{LaMnO}_{3-\delta}$ films grown under oxygen pressures of (a) 10 Pa, (b) 5×10^{-1} Pa, (c) 5×10^{-2} Pa, (d) 5×10^{-3} Pa, and (e) 5×10^{-4} Pa; (f) the oxygen-pressure-dependent c -axis lattice constant deduced from the SXR D patterns. The vertical dot line denotes the (001) peaks of SNT0.

increase of the concentration of oxygen vacancies in $\text{LaMnO}_{3-\delta}$ thin films,^{22,24} we would ascribe this modulation of the lattice constant to the effect of the oxygen vacancies in the $\text{LaMnO}_{3-\delta}$ films, which weakening the lattice

inter-atomic forces and thus inducing the increase of the volume of unit cell.

The XANES spectroscopy is a very important probe for materials.^{26–29} As an atomic probe, the XANES is strongly sensitive to the oxidation state and coordination environment of the absorbing atom. The XANES spectra of the Mn ions in the $\text{LaMnO}_{3-\delta}$ films are displayed in Fig. 2, with the different concentrations of oxygen vacancies of the $\text{LaMnO}_{3-\delta}$ films induced by the change of deposited oxygen pressure. The Mn K -edge and $L_{II,III}$ -edge spectra of the $\text{LaMnO}_{3-\delta}$ films are displayed in Figs. 2(a) and 2(b), respectively. It is well known that the Mn K -edge absorption is related to the electron transition of the $1s \rightarrow 4p$ levels, while L_{III} -edge absorption is corresponding to $2p \rightarrow 3d$ levels. The shift of the absorption edge indicates the change of the occupied band structure. It is found out from Figs. 2(a) and 2(b) that the main peaks of both the K -edge and L_{III} -edge curves of Mn ions move to the low-energy side with the decrease of the deposited oxygen pressure, which is denoted by the dashed-dotted-arrow line and vertical-solid lines on the plots, respectively. It is indicated that the average oxidation states of Mn ions decrease with the change of the concentration of oxygen vacancies with varying oxygen pressure from 10 to 5×10^{-4} Pa.²⁷ As is well known, the oxidation state of Mn ions in the stoichiometry LaMnO_3 is +3,³⁰ therefore charge transition disproportionation of the $\text{Mn}^{3+} \rightarrow \text{Mn}^{2+}$ likely occurs when the oxygen vacancies exist in the $\text{LaMnO}_{3-\delta}$ thin films, and the ratio of the $\text{Mn}^{2+}/\text{Mn}^{3+}$ should increase with increasing the oxygen vacancies. Furthermore, it can also be seen that the shape of the spectra is nearly unchanged in Figs. 2(a) and 2(b), which is sensitive to the coordination chemistry of the absorbing atom.³¹ Therefore, we believe that the coordinated environment of the Mn ions in the $\text{LaMnO}_{3-\delta}$ films is almost unchanged, consistent with the results from the SXR D analysis shown in Fig. 1. A similar changing trend of the oxidation state is shown in the spectra of K -edge and $L_{II,III}$ -edge in Fig. 2. Moreover, it is important to point out that the spectra of K -edge in Fig. 2(a) obtained by using the fluorescence measurement give the bulk absorption characteristics, while the spectra of $L_{II,III}$ -edge in Fig. 2(b) obtained by the TEY method only reflect the surface information of $\text{LaMnO}_{3-\delta}$ thin films. As a supplement and comparison, the $L_{II,III}$ -edge spectra of a series $\text{La}_{0.9}\text{Sr}_{0.1}\text{MnO}_3$ (LSMO)/SNT0 films deposited under the different oxygen pressures of 1×10^{-1} , 1×10^{-2} , 1×10^{-3} , and 4×10^{-4} Pa are also shown in Fig. 2(c). It can be

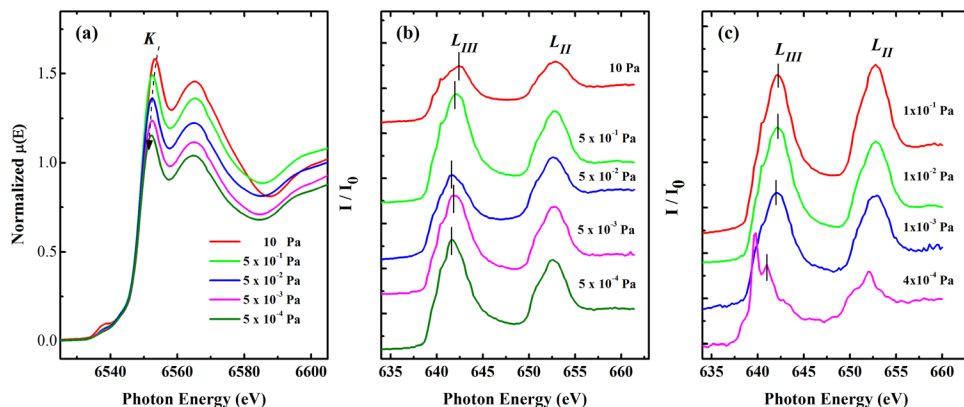


FIG. 2. The XANES spectra of the $\text{LaMnO}_{3-\delta}$ films grown under different oxygen pressures: (a) the K -edge and (b) the $L_{II,III}$ -edge spectra of Mn ions; (c) The $L_{II,III}$ -edge spectra of Mn ions in LSMO films. The dashed-dotted arrow line in (a) denotes the variation trend of the main peaks of the K -edge of Mn ions, and the vertical solid lines in (b) and (c) stand for the peak positions of the L_{III} -edge spectra of Mn ions.

concluded that the oxidation state of Mn ions has the same changing trend as that of $\text{LaMnO}_{3-\delta}$ films with various deposited oxygen pressure. It should be noted that the XANES line shape of the LSMO film of 4×10^{-4} Pa is different from the other lines displayed in Fig. 2(c). We propose that it should come from the variation of the configuration environment of the Mn sites due to the lattice distortion caused by more oxygen vacancies in this LSMO thin film.

The magnetic properties of the $\text{LaMnO}_{3-\delta}$ films are displayed in Fig. 3. The temperature (T)-dependent magnetization (M) (100 Oe, field cooled) and the hysteresis loops (10 K) of the $\text{LaMnO}_{3-\delta}$ films are shown in Figs. 3(a) and 3(b), respectively. The Curie temperature (T_C) of these films deduced from Fig. 3(a) is plotted in Fig. 3(c). Here, T_C is the calculated value obtained by fitting the high-temperature M - T curves in Fig. 3(a). The curves in higher temperature

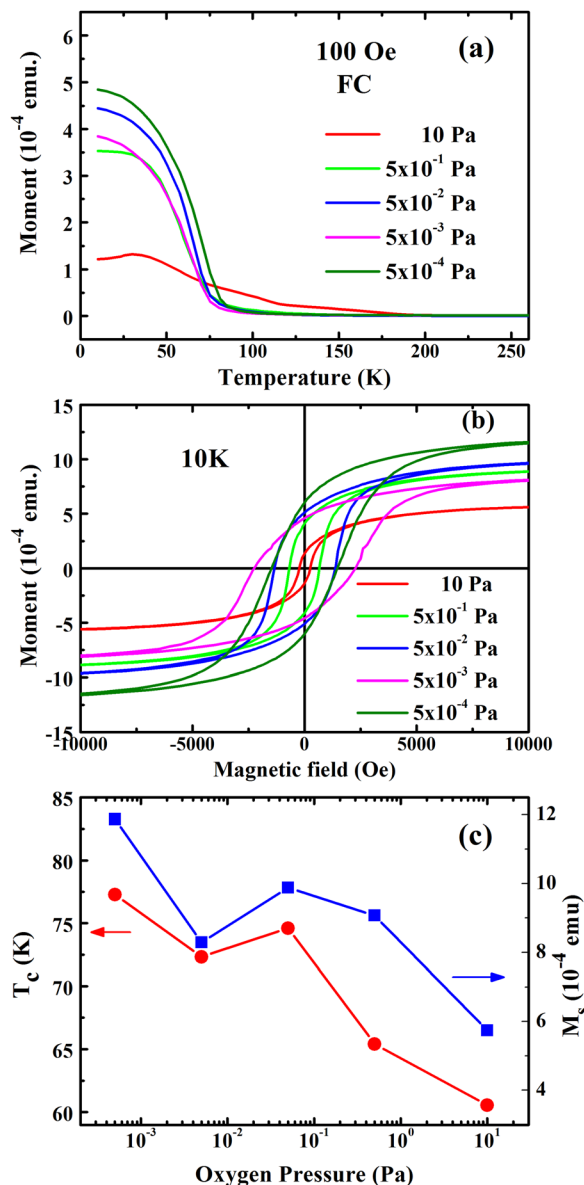


FIG. 3. (a) The temperature-dependent magnetization (100 Oe, field cooled) and (b) hysteresis loops (10 K) of the $\text{LaMnO}_{3-\delta}$ films grown under different oxygen pressures; (c) The oxygen-pressure-dependent Curie temperature (T_C) (circle-red-line) and saturation magnetization (M_s , 10 K) (square-blue-line) of the $\text{LaMnO}_{3-\delta}$ films.

can be fitted with the Curie-Weiss law $\chi = \frac{C}{T-T_C}$, where χ is the magnetic susceptibility and proportional to the magnetization, C is a material-specific Curie constant, and T is the absolute temperature. And in the same way, the saturation magnetization (M_s) of the $\text{LaMnO}_{3-\delta}$ films obtained from Fig. 3(b) is also plotted in Fig. 3(c). The ferromagnetic (FM) property was observed as shown in Fig. 3(b) in the $\text{LaMnO}_{3-\delta}$ films, which was different from the well known anti-ferromagnetic property of LaMnO_3 in bulk systems.²⁵ Both T_C and M_s increase with decreasing the deposited oxygen pressure varying from 10 to 5×10^{-4} Pa, and the residual magnetization and the coercive force also show the similar behaviors, which is not drawn in Fig. 3, but can be clearly seen in Fig. 3(b). The oxygen-pressure-dependence of T_C and M_s of the $\text{LaMnO}_{3-\delta}$ film of 5×10^{-3} Pa deviates the variation tendency, which would indicate that the magnetic structure is somehow different to the others. And this inconsistency has also been observed in the resistive switching characteristics we reported previously in Ref. 24, in which the resistance ratio of the high resistance state and the low resistance state is the largest in all $\text{LaMnO}_{3-\delta}$ thin films of 5×10^{-3} Pa we fabricated. The origin of the inconsistency remains unrevealed.

As we know, the bulk LaMnO_3 exhibits a ground-state of an A-type anti-ferromagnetic (AFM) order,²⁵ however in some special cases, the LaMnO_3 could display the FM behavior, such as in some specific oxygen-excess $\text{LaMnO}_{3+\delta}$ ceramic^{16,32} and weak tetravalent cation-doped LaMnO_3 .³³⁻³⁷ In order to interpret the ferromagnetic property of the tetravalent-cation-doped LaMnO_3 mentioned above, as well as the conductivity of the system, Mandal *et al.*³⁵ and Roy *et al.*³⁶ have suggested that the substitution of tetravalent cations in LaMnO_3 material could be considered as electron-doping, i.e., some Mn^{2+} ions in Mn^{3+} matrix, and then double exchange interaction would occur in the mixed-valent system of Mn^{2+} - Mn^{3+} . This explanation has been confirmed by the experimental evidence of the presence of Mn^{2+} in the tetravalent-cations-substituted LaMnO_3 .^{38,39} The $\text{Mn}^{2+}/\text{Mn}^{3+}$ ratio can intensely influence the strength of the double exchange interaction and then induce the variation of the ferromagnetic property. In our oxygen-deficient $\text{LaMnO}_{3-\delta}$ films, the charge transition disproportionation of the $\text{Mn}^{3+} \rightarrow \text{Mn}^{2+}$ occurs and the ratio of the $\text{Mn}^{2+}/\text{Mn}^{3+}$ increases with the decrease of the deposited oxygen pressure. We believe that the double exchange effect should exist between the Mn^{2+} and Mn^{3+} ions in our oxygen-deficient $\text{LaMnO}_{3-\delta}$ films, similar to the case between the Mn^{3+} and Mn^{4+} ions in the hole-doped manganites. With increasing the amount of the Mn^{2+} ions induced by the increase of the density of oxygen vacancies, the ratio of $\text{Mn}^{2+}/\text{Mn}^{3+}$ becomes larger, resulting in the enhancement of the double exchange interaction. Therefore, M_s and T_C increase with the decrease of the oxygen pressures from 10 to 5×10^{-4} Pa, and the residual magnetization increases as well.

The I - V curves in Fig. 4 show the transport property of the $\text{LaMnO}_{3-\delta}/\text{SNT0}$ heterostructures deposited under different oxygen pressures. With the decrease of the deposited oxygen pressure, the conductivity of the films becomes obviously larger. This enhancement of transport property would also be explained by the enhanced double exchange

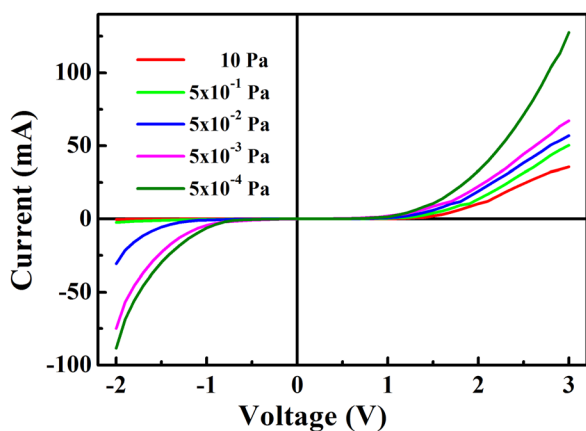


FIG. 4. The I - V curves of $\text{LaMnO}_{3-\delta}$ films grown under different oxygen pressures of 10 Pa (red-line), 5×10^{-1} Pa (green-line), 5×10^{-2} Pa (blue-line), 5×10^{-3} Pa (magenta-line), and 5×10^{-4} Pa (olive-line).

interaction in the $\text{LaMnO}_{3-\delta}$ layer of the $\text{LaMnO}_{3-\delta}/\text{SNT0}$ junctions due to the occurrence of the charge transition disproportionation of the $\text{Mn}^{3+} \rightarrow \text{Mn}^{2+}$. The enhancement of the double exchange effect would induce the rapidly increase of the conductivity electrons with the increase of the concentration of oxygen vacancies and then give rise to the larger electronic conductivities.³⁴ In the other hand, the oxygen vacancies are double donor defects in transition metal oxides;⁴⁰ therefore, the carrier density in the $\text{LaMnO}_{3-\delta}$ films would increase abundantly with increasing the oxygen vacancies induced by the decrease of deposited oxygen pressure. The electric conductivities thereby greatly enhance with decreasing the oxygen pressure.

In conclusion, the magnetic and transport properties of the $\text{LaMnO}_{3-\delta}$ films on the SNT0 substrate fabricated under various oxygen pressures have been systematically investigated. The oxygen-deficient $\text{LaMnO}_{3-\delta}$ thin films are found at the FM phase, and the Curie temperature and the saturation magnetization of the films increase with decreasing the deposited oxygen pressure. The electronic conductivities of the $\text{LaMnO}_{3-\delta}/\text{SNT0}$ heterojunctions also enhance with the increase of the oxygen vacancies. The valence state of the Mn ions has been investigated by synchrotron radiation techniques, and the results of the XANES spectra of the K -edge and the $L_{II,III}$ -edge spectra of Mn ions indicate that the charge transition disproportionation of the $\text{Mn}^{3+} \rightarrow \text{Mn}^{2+}$ occurs in the oxygen-deficient $\text{LaMnO}_{3-\delta}$ thin films and the ratio of the $\text{Mn}^{2+}/\text{Mn}^{3+}$ increases with the decrease of the deposited oxygen pressure. We believe that the change of the magnetism originates from the double exchange effect between the Mn^{2+} and Mn^{3+} ions, and the enhancements of the magnetic properties and electronic conductivities result from the enlargement of the ratio of $\text{Mn}^{2+}/\text{Mn}^{3+}$ ions with the decrease of the deposited oxygen pressure.

This work was supported by the National Basic Research Program of China (Nos. 2012CB921403 and 2013CB328706) and the National Natural Science Foundation of China (No. 11134012). The SXRD and the XANES measurements were supported by Shanghai Synchrotron Radiation Facility (SSRF).

- ¹J. J. Yang, M. D. Pickett, X. M. Li, D. A. A. Ohlberg, D. R. Stewart, and R. S. Williams, *Nat. Nanotechnol.* **3**, 429 (2008).
- ²A. Sawa, *Mater. Today* **11**, 28 (2008).
- ³K. Vanheusden, W. L. Warren, C. H. Seager, D. R. Tallant, J. A. Voigt, and B. E. Gnade, *J. Appl. Phys.* **79**, 7983 (1996).
- ⁴M. J. Zheng, L. D. Zhang, G. H. Li, and W. Z. Shen, *Chem. Phys. Lett.* **363**, 123 (2002).
- ⁵S. C. Lyu, Y. Zhang, H. Ruh, H. J. Lee, H. W. Shim, E. K. Suh, and C. J. Lee, *Chem. Phys. Lett.* **363**, 134 (2002).
- ⁶D. C. Kundaliya, S. B. Ogale, S. E. Lofland, S. Dhar, C. J. Metting, S. R. Shinde, Z. Ma, B. Varughese, K. V. Ramanujachary, L. Salamanca-Riba, and T. Venkatesan, *Nature Mater.* **3**, 709 (2004).
- ⁷J. M. D. Coey, A. P. Douvalis, C. B. Fitzgerald, and M. Venkatesan, *Appl. Phys. Lett.* **84**, 1332 (2004).
- ⁸B. Yoon, H. Hakkinen, U. Landman, A. S. Worz, J. M. Antonietti, S. Abbet, K. Judai, and U. Heiz, *Science* **307**, 403 (2005).
- ⁹H. J. Kang, P. C. Dai, B. J. Campbell, P. J. Chupas, S. Rosenkranz, P. L. Lee, Q. Z. Huang, S. L. Li, S. Komiya, and Y. Ando, *Nature Mater.* **6**, 224 (2007).
- ¹⁰I. Zeljkovic, Z. J. Xu, J. S. Wen, G. D. Gu, R. S. Markiewicz, and J. E. Hoffman, *Science* **337**, 320 (2012).
- ¹¹A. S. Moskvina, *Phys. Rev. B* **79**, 115102 (2009).
- ¹²T. Mertelj, D. Kuščer, M. Kosec, and D. Mihailovic, *Phys. Rev. B* **61**, 15102 (2000).
- ¹³I. Loa, P. Adler, A. Grzechnik, K. Syassen, U. Schwarz, M. Hanfland, G. Kh Rozenberg, P. Gorodetsky, and M. P. Pasternak, *Phys. Rev. Lett.* **87**, 125501 (2001).
- ¹⁴P. Mondal, D. Bhattacharya, P. Choudhury, and P. Mandal, *Phys. Rev. B* **76**, 172403 (2007).
- ¹⁵L. Ghivelder, I. A. Castillo, M. A. Gusmao, J. A. Alonso, and L. F. Cohen, *Phys. Rev. B* **60**, 12184 (1999).
- ¹⁶R. Laiho, K. G. Lisunov, E. Lahderanta, P. A. Petrenko, J. Salminen, V. N. Stamov, Y. P. Stepanov, and V. S. Zakhvalinskii, *J. Phys. Chem. Solids* **64**, 2313 (2003).
- ¹⁷J. Topfer and J. B. Goodenough, *J. Solid State Chem.* **130**, 117 (1997).
- ¹⁸A. N. Pirogov, A. E. Teplykh, V. I. Voronin, A. E. Kar'kin, A. M. Balagurov, V. Y. Pomyakushin, V. V. Sikolenko, A. N. Petrov, V. A. Cherepanov, and E. A. Filonova, *Phys. Solid State* **41**, 91 (1999).
- ¹⁹Q. Huang, A. Santoro, J. W. Lynn, R. W. Erwin, J. A. Borchers, J. L. Peng, and R. L. Greene, *Phys. Rev. B* **55**, 14987 (1997).
- ²⁰H. Sawada, Y. Morikawa, K. Terakura, and N. Hamada, *Phys. Rev. B* **56**, 12154 (1997).
- ²¹M. C. Sanchez, G. Subias, J. Garcia, and J. Blasco, *Phys. Rev. Lett.* **90**, 045503 (2003).
- ²²A. Y. Zuev and D. S. Tsvetkov, *Solid State Ionics* **181**, 557 (2010).
- ²³R. Cortes-Gil, A. Arroyo, L. Ruiz-Gonzalez, J. M. Alonso, A. Hernandez, J. M. Gonzalez-Calbet, and M. Vallet-Regi, *J. Phys. Chem. Solids* **67**, 579 (2006).
- ²⁴Z. T. Xu, K. J. Jin, L. Gu, Y. L. Jin, C. Ge, C. Wang, H. Z. Guo, H. B. Lu, R. Q. Zhao, and G. Z. Yang, *Small* **8**, 1279 (2012).
- ²⁵J. M. D. Coey, M. Viret, and S. Von Molnar, *Adv. Phys.* **48**, 167 (1999); Y. Tokura and Y. Tomioka, *J. Magn. Magn. Mater.* **200**, 1 (1999); A.-M. Haghiri-Gosnet and J.-P. Renard, *J. Phys. D: Appl. Phys.* **36**, R127 (2003).
- ²⁶J. G. Chen, *Surf. Sci. Rep.* **30**, 1 (1997).
- ²⁷M. Abbate, F. M. F. de Groot, J. C. Fuggle, A. Fujimori, Y. Tokura, Y. Fujishima, O. Strebel, M. Domke, G. Kaindl, J. van Elp, B. T. Thole, G. A. Sawatzky, M. Sacchi, and N. Tsuda, *Phys. Rev. B* **44**, 5419 (1991).
- ²⁸M. Wilke, F. Farges, P. E. Petit, G. E. Brown, and F. Martin, *Am. Mineral.* **86**, 714 (2001).
- ²⁹K. Shinoda, S. Suzuki, K. Yashiro, J. Mizusaki, T. Uruga, H. Tanida, H. Toyokawa, Y. Terada, and M. Takagaki, *Surf. Interface Anal.* **42**, 1650 (2010).
- ³⁰M. Abbate, F. M. F. de Groot, J. C. Fuggle, A. Fujimori, O. Strebel, F. Lopez, M. Domke, G. Kaindl, G. A. Sawatzky, M. Takano, Y. Takeda, H. Eisaki, and S. Uchida, *Phys. Rev. B* **46**, 4511 (1992).
- ³¹F. M. F. de Groot, J. C. Fuggle, B. T. Thole, and G. A. Sawatzky, *Phys. Rev. B* **41**, 928 (1990).
- ³²P. A. Joy, C. R. Sankar, and S. K. Date, *J. Phys.: Condens. Matter* **14**, 4985 (2002).
- ³³E. J. Guo, L. Wang, Z. P. Wu, H. B. Lu, K. J. Jin, and J. Gao, *J. Appl. Phys.* **110**, 113914 (2011).

- ³⁴W. Lu, Y. Sun, B. Zhao, X. Zhu, and W. Song, *Phys. Rev. B* **73**, 174425 (2006).
- ³⁵P. Mandal and S. Das, *Phys. Rev. B* **56**, 15073 (1997).
- ³⁶S. Roy and N. Ali, *J. Appl. Phys.* **89**, 7425 (2001).
- ³⁷G. T. Tan, S. Dai, P. Duan, Y. L. Zhou, H. B. Lu, and Z. H. Chen, *Phys. Rev. B* **68**, 014426 (2003).
- ³⁸C. Mitra, Z. Hu, P. Raychaudhuri, S. Wirth, S. I. Csiszar, H. H. Hsieh, H. J. Lin, C. T. Chen, and L. H. Tjeng, *Phys. Rev. B* **67**, 092404 (2003).
- ³⁹E. Beyreuther, S. Grafström, L. M. Eng, C. Thiele, and K. Dörr, *Phys. Rev. B* **73**, 155425 (2006).
- ⁴⁰D. A. Muller, N. Nakagawa, A. Ohtomo, J. L. Grazul, and H. Y. Hwang, *Nature* **430**, 657 (2004).